SLAC–PUB–7215
December 1996

A Topological Vertex Reconstruction Algorithm for Hadronic Jets*

David J. Jackson
Stanford Linear Accelerator Center,
Stanford University, Stanford, CA 94309

Permanent address: Rutherford Appleton Laboratory,
Chilton, Didcot, Oxfordshire OX11 0QX, England

E-mail: djackson@slac.stanford.edu

Abstract

The algorithm described reconstructs a set of topological vertices each associated with an independent subset of the charged tracks in a hadronic jet. Vertices are reconstructed by associating tracks with 3D spatial regions according to a vertex probability function which is based on the trajectories and position resolution of the tracks. SLD data is used to illustrate the performance of the algorithm with emphasis on the application to $Z^0 \to b\overline{b}$ events.

To appear in *Nuclear Instruments and Methods*

*Work supported by the UK Particle Physics and Astronomy Research Council and Department of Energy contract DE–AC03–76SF00515.

1 Introduction

A hadronic jet containing weakly decaying hadrons is composed of particles with differing origins. A charged track may be produced at either the jet origin, i.e. the primary vertex, or at a hadronic decay vertex. If the spatial separation of the true vertices is not significantly greater than the tracking resolution then the vertices are generally not easily identified and ambiguities arise in associating tracks with vertices. The technique described here is designed to optimise the vertex reconstruction performance in such an environment. This topological vertex finding algorithm has been developed for data collected by the SLC Large Detector (SLD) at the Stanford Linear Collider (SLC). The excellent 3D resolution of the SLD pixel vertex detector (VXD2) makes the efficient reconstruction of decay vertices in the hadronic jets produced by Z^0 decays possible.

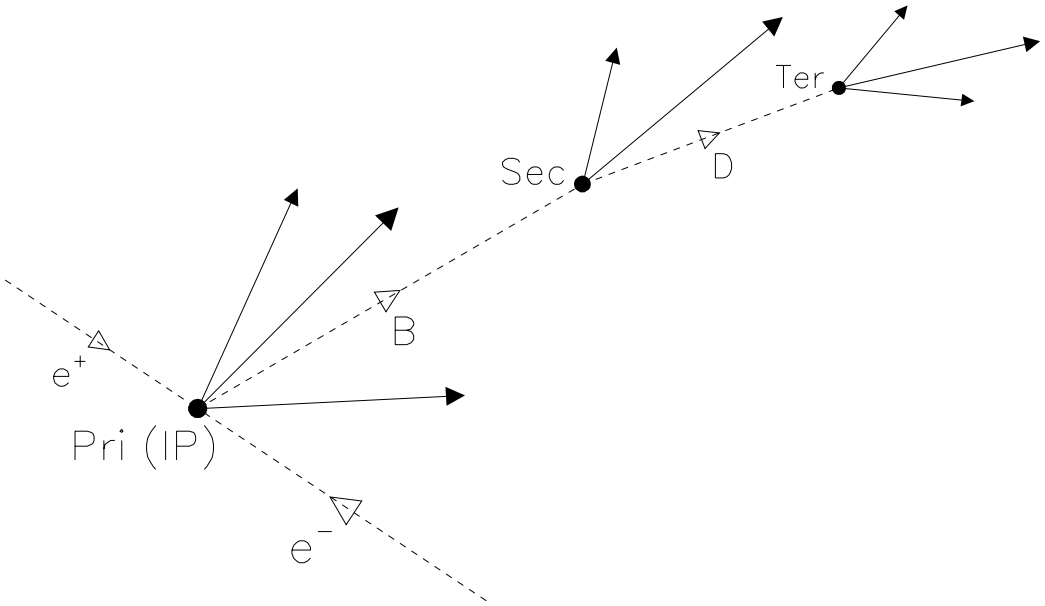

Figure 1: Tracks produced (solid lines) in one hemisphere of a $Z^0 \to b\bar{b}$ event.

Since the mass of the Z^0 is significantly greater than the mass of the quark pairs it can decay into, the events can be divided into two hemispheres. For a $Z^0 \to b\bar{b}$ event a B hadron decay is expected in each hemisphere (except

in the case of hard gluon radiation). Such a hemisphere from a $Z^0 \rightarrow b\overline{b}$ event is represented in fig. 1. In this case the tracks originate from three vertices; the fragmentation tracks from the primary vertex at the e^+e^- IP (Interaction Point), tracks from the secondary B hadron decay and tracks from the tertiary D hadron decay. The reconstruction of vertices formed by the tracks from the weakly decaying hadrons allow the properties of such hadrons to be studied.

The decay lengths are typically shorter than the distance to the first layer of the vertex detector. Hence no information about the location of the track origin longitudinal to the trajectory is measured, while the transverse position is measured to within the resolution of the vertex detector. In other words there is some degree of uncertainty concerning the transverse origin of each track while the longitudinal origin of the track is completely undetermined. However, by combining the tracking information for the set of tracks in the jet the topological vertex structure may be identified. The following section describes this procedure.

2 An Algorithm to Resolve Vertices

The philosophy adopted is to search for vertices in 3D co-ordinate space rather than by forming vertices from all track combinations (the latter becomes impracticable for events with high track multiplicity). This search is based on a function $V(\mathbf{r})$ which quantifies the relative probability of a vertex at location $\mathbf{r}$. The first step is to obtain from the helix parameters (or, in general, the relevant trajectory parameters) of each track i a function $f_i(\mathbf{r})$ representing a Gaussian probability tube for the track trajectory,

$$f_i(\mathbf{r}) = \exp\left\{-\frac{1}{2}\left[\left(\frac{x' - (x'_0 + \kappa y'^2)}{\sigma_T}\right)^2 + \left(\frac{z - (z_0 + \tan(\lambda)y')}{\sigma_L}\right)^2\right]\right\}, \quad (1)$$

where the x, y co-ordinates have been transformed into x', y' for each track such that the track momentum is parallel to the positive y' co-ordinate axis in the xy plane at the point of closest approach to the IP (x'_0, z_0 are the x', z co-ordinates at this point). The Gaussian tube is represented by the

parallel dotted lines in fig. 2. The first term inside the exponential includes a parabolic approximation to the circular track trajectory in the xy plane, where κ is determined from the magnetic field and the particle charge and transverse momentum. The trajectory is propagated into the third dimension z via the helix parameter λ in the second term of the exponential. The quantities σ_T and σ_L are the measurement errors for the track in the xy plane and z direction respectively. In general these quantities are a function of location since the track trajectory is known more precisely close to a hit in the vertex detector. If the distance to the first layer of the vertex detector is large compared with the region of physics interest close to the IP then σ_T and σ_L may be treated as constants, measured at the point of closest approach of the track to the IP.

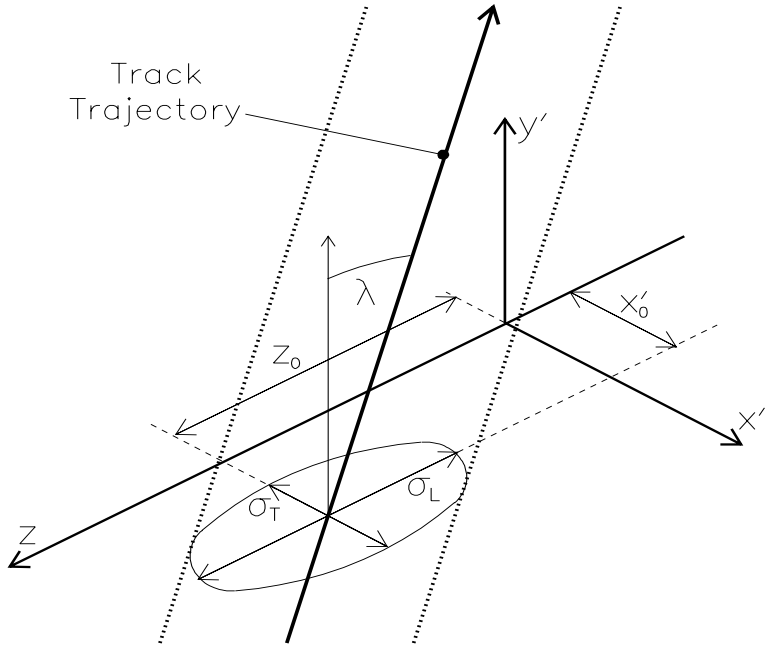

Figure 2: Construction of the Gaussian tube $f_i(\mathbf{r})$ for each track i.

In order ultimately to decide which of the vertices is the primary and to constrain it to be consistent with the IP position a further function $f_0(\mathbf{r})$ is introduced describing the IP location and uncertainty. For SLD it is simply a 3D unnormalized Gaussian ellipsoid centred on the IP with $\sigma_X = \sigma_Y =$

7μm and σ_Z=70μm reflecting the uncertainty in the position of the IP (see section 5.1). The IP function is analogous to $f_i(\mathbf{r})$ for the tracks and it is treated in a similar way. The notation 'track-IP' will be used when a statement refers to both the track and the IP functions. The weight given to $f_0(\mathbf{r})$ in calculating $V(\mathbf{r})$ may be modified by a tunable parameter (see section 4). Using the function $f_0(\mathbf{r})$ improves the vertex finding performance by introducing information additional to that contained in the jet of tracks being considered (see section 5.1).

The Gaussian track functions are left unnormalized in order that the vertex function introduced below is sensitive to track multiplicity as a function of $\mathbf{r}$. The relative probability of a vertex at $\mathbf{r}$ is defined taking into account that the value of $f_i(\mathbf{r})$ must be significant for at least two tracks-IP in this region. A smooth, continuous function is desired so that its maxima may be found. These requirements result in the form:

$$V(\mathbf{r}) = \sum_{i=0}^{N} f_i(\mathbf{r}) - \frac{\sum_{i=0}^{N} f_i^2(\mathbf{r})}{\sum_{i=0}^{N} f_i(\mathbf{r})}. \qquad (2)$$

where N is the number of tracks. The first term on the rhs is a measure of the multiplicity and degree of overlap of the track-IP probability functions and hence a measure of the probability that at least some of the tracks originate at $\mathbf{r}$ and hence form a vertex at this location. Due to the second term on the rhs of equation 2, $V(\mathbf{r}) \simeq 0$ in regions where $f_i(\mathbf{r})$ is significant for only one track-IP. The form of $V(\mathbf{r})$ can be modified to fold in known physics information about probable vertex locations (see section 4).

An example of the xy projection of $\sum_{i=0}^{N} f_i(\mathbf{r})$ and $V(\mathbf{r})$ is shown in fig. 3(a) and 3(b) respectively. These plots are obtained by integrating the function over the third dimension z within the limits of $\pm$0.8 cm from the IP in the z direction. (This 2D projection is for diagrammatic convenience only). The hemisphere of tracks chosen for this plot is taken from an SLD Monte Carlo $Z \rightarrow b\overline{b}$ event in which the jet momentum is directed from left to right in fig. 3. The trajectories of individual tracks can be seen in fig. 3(a). The regions where vertices are probable can be seen from the distribution of $V(\mathbf{r})$ in fig. 3(b). In this case the algorithm resolved the hemisphere into two vertices, i.e. the primary vertex and a secondary. The peak in $V(\mathbf{r})$ produced by the primary can be seen in fig. 3(b) at $X = Y = 0$, the secondary peak is displaced to the right of the IP by $\sim$0.15 cm. A subset of the tracks-IP is

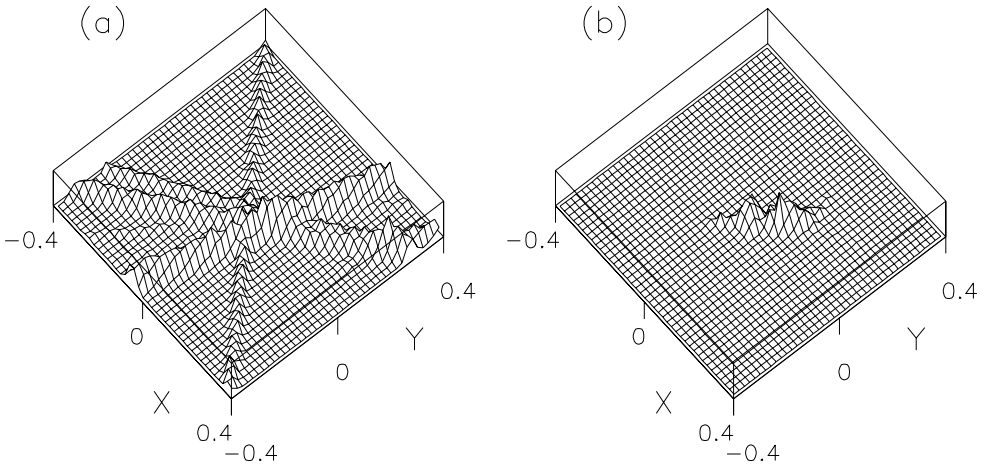

Figure 3: The track (a) and vertex (b) functions projected onto the xy plane (cm).

associated with each of the resolved maxima of $V(\mathbf{r})$ to identify the set of reconstructed vertices.

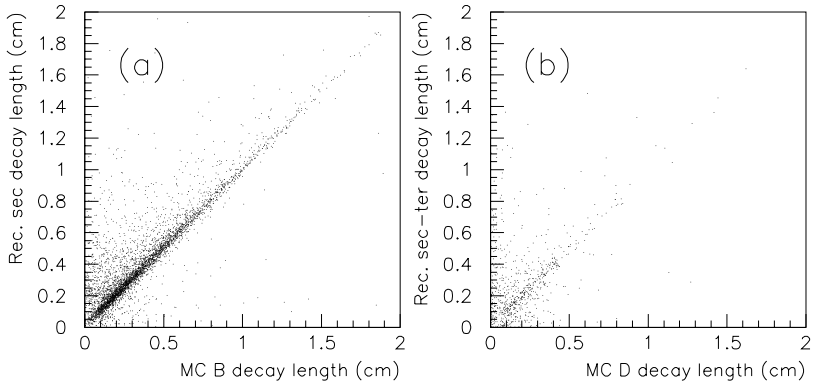

Figure 4: Reconstruction of heavy hadron decay lengths in $Z^0 \to b\bar{b}$ events.

Fig. 4 shows the reconstructed decay lengths from SLD $Z^0 \to b\bar{b}$ Monte Carlo hemispheres for (a) the B hadron decay length in which one secondary vertex has been found, and (b) the D decay length in events for which a tertiary vertex is also reconstructed. The asymmetry of the scatter plot about the diagonal in fig. 4(a) is the effect of the cascade charm decay augmenting

the reconstructed B decay length. To fully reconstruct the B to D decay chain for fig. 4(b) requires at least two charged tracks to be well measured from both hadron decays and that all three vertices (including the primary) be well separated, the efficiency and purity of the full reconstruction is therefore somewhat lower than that for finding a single displaced vertex. However, the algorithm will attempt to fully reconstruct *all* physics vertices in the jet of tracks. A vertex can be reconstructed if it is spatially 'resolved' from other vertices.

The criterion used for resolving maxima of $V(\mathbf{r})$ is the following, it is used wherever terms like 'resolved' appear in this paper. The two locations $\mathbf{r_1}$ and $\mathbf{r_2}$ are said to be resolved if:

$$\frac{\min\{V(\mathbf{r}) : \mathbf{r} \in \mathbf{r_1} + \alpha(\mathbf{r_2} - \mathbf{r_1}), 0 \leq \alpha \leq 1\}}{\min\{V(\mathbf{r_1}), V(\mathbf{r_2})\}} < R_0, \tag{3}$$

where $\min\{V(\mathbf{r_1}), V(\mathbf{r_2})\}$ is the lower of the two values and the numerator in equation 3 is the minimum of $V(\mathbf{r})$ on a straight line joining $\mathbf{r_1}$ and $\mathbf{r_2}$; in practice $V(\mathbf{r})$ is determined for a finite number of points on this line. The number of vertices found will depend on the cut value, $0 \leq R_0 \leq 1$, chosen. The value of R_0 as well as the maximum χ^2 contribution of a track to a vertex, χ^2_0 (discussed below), are tunable parameters.

It is not necessary to search the whole of the 3D space in the region of physics interest in order to find the maxima of $V(\mathbf{r})$. Since at least two of the functions $f_i(\mathbf{r})$ must contribute to a maximum in $V(\mathbf{r})$ the spatial locations of the maxima of $f_i(\mathbf{r})f_j(\mathbf{r})$ are first found by direct calculation. For each of these spatial points the corresponding 3D maximum is found in $V(\mathbf{r})$ iteratively in the proximity of the $f_i(\mathbf{r})f_j(\mathbf{r})$ maximum. By initializing this iterative procedure at the calculated maxima of $f_i(\mathbf{r})f_j(\mathbf{r})$ the effective 3D search area is much smaller than the potential region of physics vertices and all the maxima in $V(\mathbf{r})$ are found. These maxima are clustered together to form candidate vertex regions using the resolution criterion. If a maximum in $V(\mathbf{r})$ which was found near the maximum of $f_i(\mathbf{r})f_j(\mathbf{r})$ is included in such a cluster, then the tracks i and j belong to the corresponding vertex candidate. If the IP function ($i = 0$) is included in the cluster then the vertex is identified as the primary. This procedure is described in more detail in the following paragraphs.

In a jet of N tracks the $\frac{1}{2}N(N+1)$ locations $\mathbf{r}_{ij}$ of the $f_i(\mathbf{r})f_j(\mathbf{r})$ maxima ($i, j = 0 \ldots N$, $i \neq j$) are found and retained if both tracks-IP pass the cut

$\chi^2 < \chi^2_0$ at $\mathbf{r}_{ij}$. The track-IP k is associated with the spatial point having the greatest value of $V(\mathbf{r}_{kj})$ (obtained for $j = 0 \ldots k-1, k+1 \ldots N$). In addition, for each track, in order of decreasing values of $V(\mathbf{r}_{kj})$ further locations are retained in association with the track if they are resolved from locations already associated with the track. The resolution criterion is used here since there is no need to associate a track with two spatial points that will ultimately be clustered into the same vertex region. In general each track may therefore be associated with 0 to N spatial locations although in practice this number is much less than N. Allowing the tracks to be associated with more than one spatial region enhances the vertex finding efficiency; it also leads to ambiguities in assigning a track to a unique vertex which must later be resolved. The IP is associated with only one spatial point (i.e. the location of the highest $V(\mathbf{r}_{0j})$).

An iterative procedure in xyz space transforms each of the $\mathbf{r}_{ij}$ (maxima of $f_i(\mathbf{r})f_j(\mathbf{r})$) into the location of the nearest maximum in $V(\mathbf{r})$. The transformed spatial points $\mathbf{r}_{ij}$ are then clustered into separate regions of 3D space according to the resolution criterion. The spatial point with the highest $V(\mathbf{r}_{ij})$ is taken as the seed of the first cluster. All spatial points *not* resolved from this seed location according to equation 3 are added to the cluster. Any remaining spatial points are added to the cluster if they are not resolved from *any* spatial point in the cluster; this procedure continues until no further locations are added to the cluster. Of the remaining unclustered spatial points the one with the highest $V(\mathbf{r}_{ij})$ is now taken as the seed of the second cluster and the above procedure is repeated. This clustering algorithm of taking a seed location and adding unresolved locations continues until no spatial points remain unclustered. The resulting number of clusters (typically ~ 4 for a jet at SLD in which a B hadron decays at > 0.1 cm) is equal to the number of candidate vertices in the jet.

The candidate vertices are formed by associating the resolved spatial clusters with a subset of the N tracks and the IP via the set spatial points $\mathbf{r}_{ij}$ forming the cluster. Since the tracks were allowed to be associated with several resolved spatial points the subsets of tracks associated with the spatial cluster will in general not be independent. At all stages non-primary vertices are rejected if they consist of < 2 tracks (by definition). The subset of tracks in each vertex is taken in turn and fit to a common vertex. If the track with the largest χ^2 contribution to the vertex fails the cut $\chi^2 < \chi^2_0$ it is removed from the vertex, and the remaining tracks (if ≥ 2) are refit. The process

is repeated iteratively until all tracks with a bad χ^2 contribution have been trimmed away. The fit is not explicitly checked in the clustering process and the χ^2 trimming avoids vertices in the final set having a very low fit probability. Any remaining track ambiguities are decided as follows. The tracks in the vertex with the largest value of $V(\mathbf{r})$ (taken to be the highest $V(\mathbf{r}_{ij})$ in the spatial cluster forming the vertex) are fixed in that vertex and removed from any others. The remaining vertices are considered in order of decreasing values of $V(\mathbf{r})$ and at each stage the tracks still remaining in the vertex are fixed into that vertex and removed from vertices with smaller $V(\mathbf{r})$ values. This procedure uniquely assigns each track to a vertex, each of which is refit and the topological vertex finding is complete. (Alternatively, it may be desirable to retain a degree of ambiguity and associate tracks with an arbitrary number of vertices with each association being characterized by the corresponding χ^2 contribution of the track to the vertex). The vertex found to include the IP function is called the primary vertex and may be associated with any number from 1 to N tracks. If the IP does not belong to any of the resolved spatial clusters then there are no tracks in the primary vertex. The non-primary vertices are labelled (secondary, tertiary etc.) according to their distance from the IP.

3 Topological track parameters

The information obtained for each track includes the associated vertex number (unassociated tracks are classified as 'isolated') and the χ^2 contribution of the track to this vertex. Topological track parameters are defined and measured as follows. A vertex axis is formed by a straight line joining the IP to a secondary (seed) vertex, fig. 5. If several non-primary vertices are found one must be selected as the seed vertex. For example, the most significant vertex (highest value of $V(\mathbf{r})$) or the one reconstructed furthest from the IP (used in this case) may be chosen as the seed. The transverse 3D impact parameter, T, and the distance along the vertex axis to this point, L, are calculated. Tracks classified as isolated but having small values of T are likely to be associated with the decay sequence in a $Z^0 \to b\overline{b}$ event hemisphere (since the momentum of the cascade D hadron is approximately collinear with the

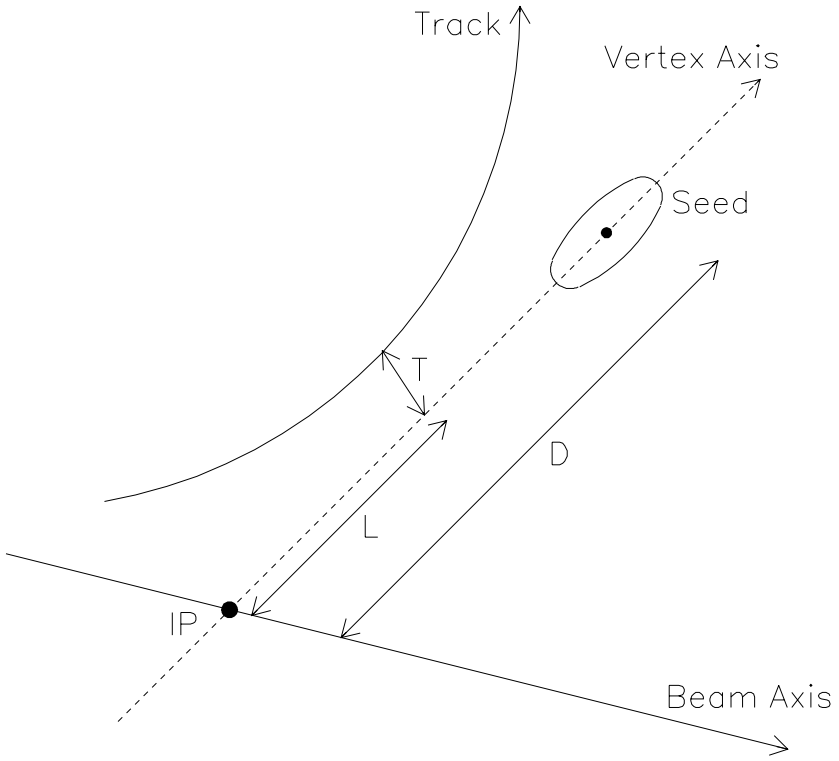

Figure 5: Impact parameter of a track to the vertex axis.

momentum of the parent B hadron). The value of L for such tracks, compared with the vertex decay length, D, locates the track position along the decay chain. The quantity L/D is plotted in fig. 6 for tracks classified as isolated but of differing Monte Carlo origins. Hence these parameters allow the possibility of reconstructing 'one-prong vertices', (e.g. a lepton 'vertex' in a semileptonic B decay) relative to a topologically reconstructed multi-prong vertex.

4 Tuning the Algorithm

In addition to R_0, equation 3, and χ_0^2 two further tunable parameters, K_{IP} and K_α are used to optimize the topological vertexing performance. The

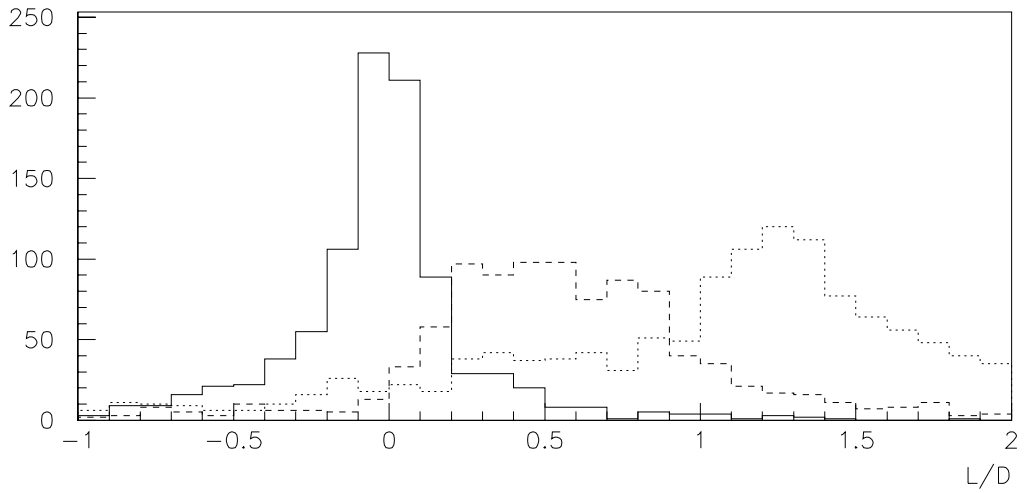

Figure 6: The ratio L/D for tracks reconstructed as isolated in $Z^0 \to b\overline{b}$ Monte Carlo events for primary (solid line), B decay (dashed line) and D decay (dotted line) tracks.

latter two parameters allow the vertex significance function $V(\mathbf{r})$ (equation 2) to be weighted in regions where real vertices are more probable. In general, $V(\mathbf{r})$ may be given a high or low weight in regions where the genuine or fake (respectively) vertex probability is expected to be high due to considerations such as physics, kinematics or geometry. The weight K_{IP} is introduced into the definition of $V(\mathbf{r})$:

$$V(\mathbf{r}) = K_{IP} f_0(\mathbf{r}) + \sum_{i=1}^{N} f_i(\mathbf{r}) - \frac{K_{IP} f_0^2(\mathbf{r}) + \sum_{i=1}^{N} f_i^2(\mathbf{r})}{K_{IP} f_0(\mathbf{r}) + \sum_{i=1}^{N} f_i(\mathbf{r})}. \tag{4}$$

Values of $K_{IP} > (<) 1.0$ mean that it is less (more) likely that secondary vertices will be found near the IP, a region where the fake vertex background is large. That is, large values of K_{IP} will enhance $V(\mathbf{r})$ at the IP and absorb more tracks into the primary vertex. In addition, the vertex function may be modified by a factor dependent upon the angular location of the spatial point $\mathbf{r}$:

$$V(\mathbf{r}) \to V(\mathbf{r}) \exp(-K_\alpha \alpha^2), \tag{5}$$

where the angle α is defined in fig. 7. The dimensions used are suitable for the SLD environment. The cylinder of radius 50 μm centred on the jet

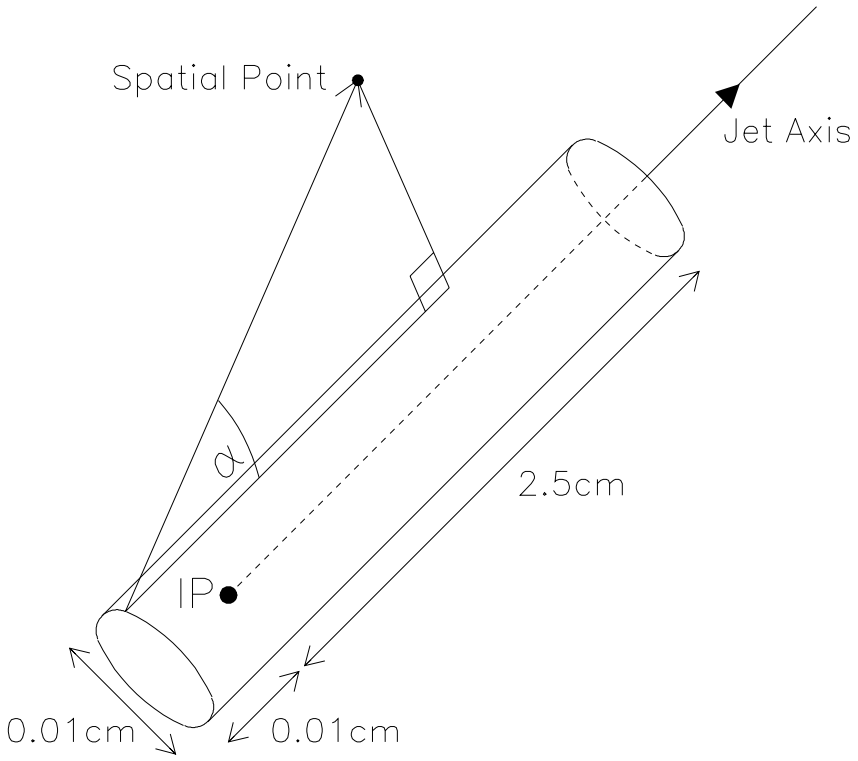

Figure 7: Construction of α, the angular displacement.

axis is constructed in order that $V(\mathbf{r})$ is not reduced in the area close to the IP. In the regions where the distance from the IP projected onto the jet axis is $< -100\mu$m or > 2.5cm, $V(\mathbf{r})$ is set equal to zero since these locations are unlikely to contain useful vertices. Fake vertices involving primary tracks diverging from the IP are more likely to occur at higher values of α than the genuine secondaries. By either a cut on the value of α for a vertex location after the vertices have been found or tuning K_α (~ 5.0 for a 45 GeV jet at SLD, in general K_α should be proportional to the jet momentum) at the input stage, the purity of the secondary vertices can be improved.

5 Performance with SLD events and VXD2

5.1 The SLD

The algorithm has been applied to data collected by the SLD (SLC Large Detector) at the SLC (Stanford Linear Collider). The excellent 3D resolution of the SLD vertex detector, as well as the availability of the SLC polarized electron beam, allow competitive results from a relatively small data sample; 150,000 hadronic Z^0 decays collected during 1993-5. The collaboration expects to accumulate an additional 500,000 highly polarized Z^0s with an upgraded vertex detector (VXD3).

A detailed description of the SLD detector can be found in Ref. [1]. The SLD vertex detector (VXD2)[2] is described briefly here. The VXD2 consists of 480 charge-coupled devices (CCDs) surrounding a 1 mm thick beryllium beam pipe with an inner radius of 25 mm. Each CCD consists of 375×578 22 μm^2 pixels. The active material is a 20 μm thick epitaxial silicon layer on a 180 μm thick silicon substrate. The CCDs are mounted on 60 alumina boards 9.2 cm long, arranged in four concentric cylinders at radii ranging from 2.9 cm to 4.1 cm. The inner (outer) cylinder covers a range of polar angles defined by $|\cos\theta| < 0.85$ (0.75). The CCDs are arranged such that a charged track will make at least two hits over the full azimuth within the polar angle acceptance. On average 2.3 CCDs are traversed by a track from the IP. The spatial resolution of VXD2 is 6 μm transverse to the beam and 7 μm along the beam direction[3].

Charged tracks found in the central (or barrel) drift chamber (CDC)[4] are linked to clusters of pixels in VXD2 by extrapolating each track and selecting the best set of associated clusters[3]. A set of clusters may not be shared by multiple tracks. The track parameters are then recalculated, accounting for multiple scattering. The track impact parameter resolutions are $11\,\mu$m and $38\,\mu$m in the $r\phi$ and rz projections respectively with an additional multiple scattering contribution of $70/p\sin^{3/2}\theta\,\mu$m in both projections, where p is expressed in GeV/c. The momentum resolution of the tracking system in the 0.6 T field of the SLD solenoid is $\left(\frac{\delta p_{\rm T}}{p_{\rm T}}\right)^2 = 0.01^2 + (0.0026\ p_{\rm T})^2$, where $p_{\rm T}$ is the track transverse momentum in GeV/c.

The SLC collides bunches of 45.6 GeV electrons and positrons accelerated

in the SLAC linac at a rate of 120 Hz. The spatial extent of the bunches at the IP is typically ≈ 0.8 μm vertically, ≈ 2.6 μm horizontally, and ≈ 700 μm longitudinally[5]. The transverse position of the SLC collision region is stable, with variations of typically 5-10 μm over time periods measured in hours. A fit to a single point in the transverse plane is made using tracks from ~ 30 successive hadronic Z^0 decays to find the spatial location of the IP [3] with an uncertainty of 7 ± 2 μm. The median z position of tracks at their point of closest approach to the IP in the xy plane is used to determine the z position of the e^+e^- interaction on an event-by-event basis. A precision of $\sim 52\mu$m on this quantity is estimated using $Z^0 \to b\bar{b}$ Monte Carlo [3].

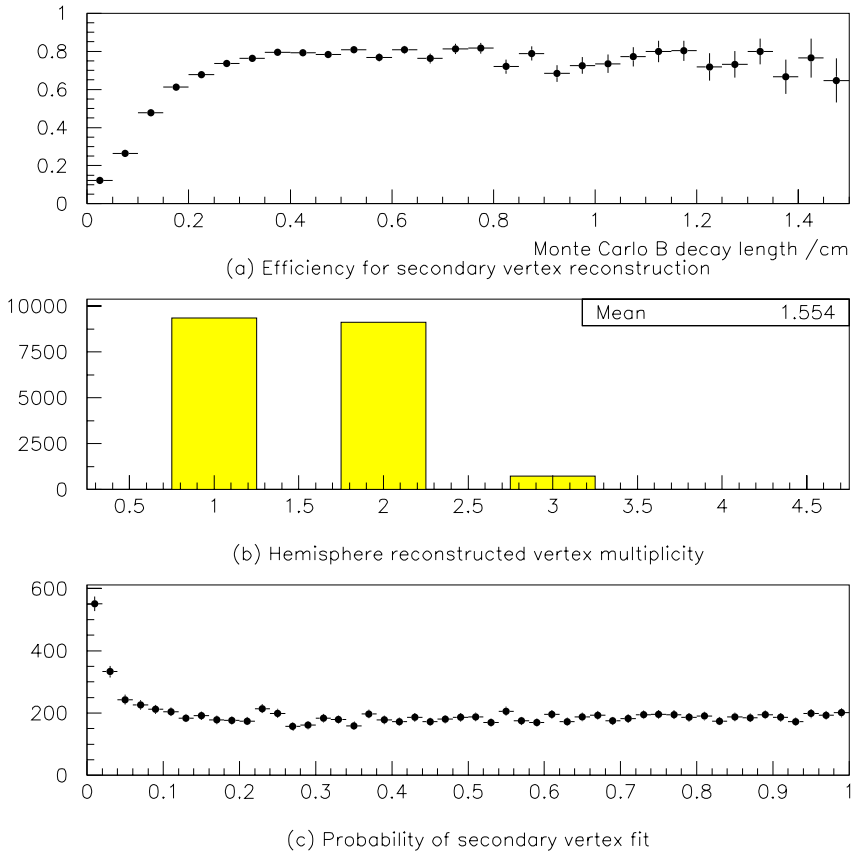

Figure 8: Vertex reconstruction in Monte Carlo $Z^0 \to b\bar{b}$ event hemispheres (a) efficiency, (b) multiplicity (c) fit probability.

5.2 Vertexing Performance

Following standard SLD event and track selection the algorithm is applied separately to the tracks in each event hemisphere. The tuning parameters are set to $R_0 = 0.6$, $\chi^2_0 = 10.0$, $K_{IP} = 1.0$, and $K_\alpha = 5.0$. Monte Carlo events generated using JETSET 7.4 [6] with the SLD detector simulated by GEANT 3.21 [7] are used to study the vertex finding efficiencies and purities. The efficiency for reconstructing a secondary vertex in a $Z^0 \to b\overline{b}$ event hemisphere is shown in fig. 8(a) as a function of the true B hadron decay length. The efficiency is lower for short B decay length since it becomes harder to resolve the secondary, from the primary, near the IP. Larger value of R_0 (equation 3) increase the vertex finding efficiency in this region, at the cost of purity. The vertex multiplicity is shown in fig. 8(b), where the '1 vertex' case means that only the primary vertex was found. The total efficiency for reconstructing a secondary vertex in a $Z^0 \to b\overline{b}$ event hemisphere is about 50% (in charm and light quark hemispheres it is about 15% and 3% respectively). The probability of the secondary vertex fit is shown in fig. 8(c). The size of the peak near zero probability depends directly on the input value of χ^2_0, the maximum χ^2 contribution of a track to a vertex. Otherwise the probability spectrum is flat, as expected for genuine vertices. The purity of the vertices, that is the likelihood of correctly associating a track with a vertex is shown in table 1 for the case in which a secondary only (two vertex case) and a secondary plus tertiary (three vertex case) is reconstructed.

Monte Carlo track origin	Reconstructed track-vertex association						
	Two vertex case			Three vertex case			
	pri	sec	iso	pri	sec	ter	iso
Primary	93	3	4	77	16	3	4
B decay	14	80	6	6	65	25	4
D decay	8	82	10	3	25	68	4

Table 1: Purity of reconstructed track-vertex association (%).

As shown above (fig. 6) the isolated tracks may be attached to the seed vertex via a cut on the quantity L/D. The selection of tracks resulting from the B decay chain is optimized by attaching all non-seed tracks with L/D>0.3

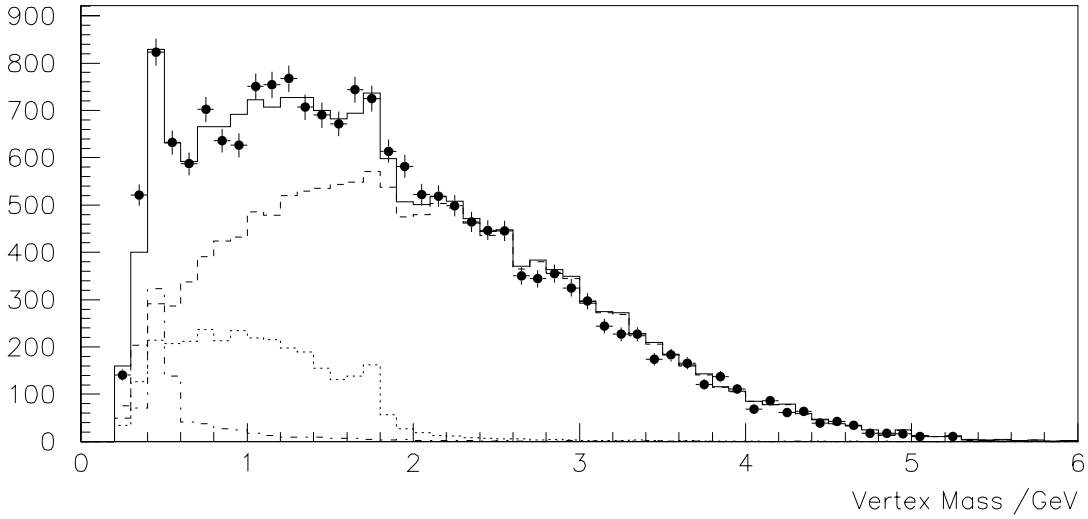

Figure 9: Reconstructed secondary vertex mass for SLD 1994-5 data (points) and Monte Carlo (solid line) composed of $Z^0 \to b\overline{b}$ events (dashed lines), $Z^0 \to c\overline{c}$ events (dotted line) and light quark events (dash-dotted line) .

(including tracks initially classified as primary). The invariant mass spectrum of this set of tracks (tracks in the seed vertex or passing L/D>0.3) is shown in fig. 9 for vertices reconstructed at a distance greater than 0.1cm from the IP. The vertex mass is calculated by assuming that each track has the mass of a pion. The Monte Carlo event sample used in this plot is 2.5 times larger than the 1994-5 data sample. A K^0_S mass peak is visible around 0.5 GeV/c^2. For the B and D decays the reconstructed mass is generally less than that of the decaying hadron due to the missing neutral energy. The mass spectrum for the $Z^0 \to c\overline{c}$ events falls rapidly above the D hadron mass (around 2 GeV/c^2) leaving a purer sample of $Z^0 \to b\overline{b}$ events which are reconstructed up to the B hadron mass around 5 GeV/c^2. This sample of vertices with mass > 2GeV/c^2 has a high purity of tracks from the B decay chain such that the total charge of these tracks tags neutral or charged B decays. This charge reconstruction has been used at SLD to measure the ratio of the B^0 and B^+ lifetimes [8].

References

[1] SLD Design Report, SLAC-REPORT-273, May 1984.

[2] G.D. Agnew et al., "Design and Performance of the SLD Vertex Detector, a 120 MPixel Tracking System", Proceedings of the XXVI International Conference on High Energy Physics, Dallas, Texas, 6–12 August, 1992, M. Strauss et al., "Performance of the SLD CCD Pixel Vertex Detector and Design of an Upgrade," Proceedings of the 27th International Conference on High Energy Physics, Glasgow, Scotland, July 20-27, 1994.

[3] K. Abe et al., "Measurements of R_b with Impact Parameters and Displaced Vertices", *Phys. Rev.* **D53**, 1023 (1996).

[4] M.D. Hildreth et al., "Performance of the SLD Central Drift Chamber", *IEEE Trans. Nucl. Sci.* **42**, 451 (1995).

[5] M. Breidenbach, "SLC and SLD – Experimental Experience with a Linear Collider", in Waikoloa 1993, Proceedings, Physics and Experiments with Linear e+ e- Colliders, vol. 1, pp. 30-45, and SLAC-PUB-6313 (August 1993).

[6] T. Sjöstrand, CERN-TH-7112-93, Feb. 1994.

[7] R. Brun *et al.*, CERN-DD/EE/84-1, 1989.

[8] K. Abe et al., "Preliminary Measurements of B^0 and B^+ Lifetimes at SLD", SLAC-PUB-6972, August 1995.